



Numerical simulation of explosively driven metal by material point method[☆]

Y.P. Lian^a, X. Zhang^{a,b,*}, X. Zhou^c, S. Ma^a, Y.L. Zhao^c

^aSchool of Aerospace, Tsinghua University, AML, Beijing 100084, China

^bState Key Laboratory of Structural Analysis for Industrial Equipment, Dalian University of Technology, Dalian 116024, China

^cBeijing Institute of Special Engineering Design and Research, Beijing 100028, China

ARTICLE INFO

Article history:

Received 17 February 2010

Received in revised form

23 October 2010

Accepted 25 October 2010

Available online 11 November 2010

Keywords:

Material point method

Detonation

Explosive-driven flyer

Large deformation

ABSTRACT

The material point method (MPM) fully takes the advantages of both Lagrangian method and Eulerian method, and can be capable of simulating high explosive explosion problems and impact problems involving large deformation and multi-material interaction of different phases. In this paper, MPM is extended to simulate the explosively driven metal problems, and two typical explosive/metal configurations, open-faced sandwich and flat sandwich, are analyzed in detail using MPM, and numerical results are compared with Gurney solution and its corrections. Based on our MPM results, a new correction to Gurney solution is proposed to account for the lateral effects for flat sandwich configuration. MPM provides a powerful tool for studying the explosively driven metal and other explosive problems.

© 2010 Elsevier Ltd. All rights reserved.

1. Introduction

Being one handled way to obtain an object in high speed by the release of energy from the detonation of conventional secondary explosives, explosive driven is widely used in engineering and scientific research for various motives or purposes. For example, the investigation of the fraction of energy of the explosive used to propel the fragments is very useful for the design of powerful fragmentation bomb and warhead of missile. In order to simulate the impact between aircraft and orbital, an object with hypervelocity must be provided in the laboratory, which can be driven by detonation, in the design of the space debris shields. Furthermore, the driven fragments can be used to study the dynamic behavior of materials. Therefore, theoretical and numerical investigations of the explosively driven metal are of important theoretical significance and practical value.

When an explosive surrounded by a metallic or other solid shell detonates, the outer shell is accelerated both by the initial detonation shock wave and by the expansion of the detonation gaseous products contained by the outer shell. In 1940s, a simple model to predict the terminal velocity of fragments from grenades and

artillery shells was developed by Gurney [1]. By measuring the velocities of fragments from bombs weighing as much as 3000 pounds to grenades containing as little as 1.5 ounces of a high explosive, he concluded that the governing factor to determined the final velocities of fragments was the ratio of the mass of the fragments to the mass of the explosive. Although the interaction of a detonating explosive with driving fragments is extremely complex involving detonation waves, shock waves, expanding gases, and their interrelationships, the assumptions Gurney made in this model to provide mathematical tractability are only based on energy and momentum balances with two key assumptions in its derivation, which is that a specific energy is assumed to be converted from chemical energy in the initial state to kinetic energy of the driven inert material and the detonation product gases in the final state, and those product gases have a uniform density and a linear one-dimensional velocity profile in the spatial coordinates of the system [2,3]. In spite of its simplicity, the Gurney method has been proven to give good predictions for much different casing geometry [4,5]. Henry [6] provided a comprehensive review of the Gurney method and derivation of many formulas. Gurney equations for common symmetric and asymmetric explosive/metal configurations, such as symmetrical sandwich (flat sandwich), asymmetrical sandwich, infinitely tamped sandwich, open-faced sandwich, cylindrical and imploding cylindrical charge, spherical and imploding spherical charge, have been obtained [7] as the function of the Gurney energy and the ratio of the total metal mass to the total explosive mass.

[☆] Supported by National Basic Research Program of China (2010CB832701) and National Natural Science Foundation of China (10872107).

* Corresponding author. School of Aerospace, Tsinghua University, AML, Beijing 100084, China.

E-mail address: xzhang@tsinghua.edu.cn (X. Zhang).

In fact, the Gurney model may have overestimated the flyer velocities due to its simplified assumptions which are only applicable for one-dimensional configuration [3,8,9]. Therefore, this method was further improved by others [9–12] to account for the lateral effects based on empirical correction factors or theoretical analysis. Baum et al. [11] indicated that, in the case of an unconfined charge of explosive resting on a plate, the explosive which was effective in driving the plate was the core of the explosive nearest to the plate. Therefore, the lateral edges of the explosive had to be subtracted from the total mass of explosive [7]. Fucke et al. given correction factors with regard to plate thicknesses, plate dimensions and gaps in the high explosive layer for sandwich configuration [10].

Gurney models are over simplified for low values of M/C where gas-dynamic behavior dominates, so that Gurney solutions cannot be trusted for this regime. Aziz et al. treating the driven metal as a rigid body and the gases with an ideal gas equation of state, they performed an analysis for an open-faced sandwich configuration [3,13]. Their solution should be applicable for all values of M/C because it treats the gas dynamics fully.

Gurney model and its corrections can only predict the terminal velocity of fragment for some simple configurations. They are based only on energy and momentum balances, and have nothing to do with shock waves although they play a very important role in the driving process. In contrast, numerical simulation not only can predict the terminal velocity, but also can study the whole driving process, including the expanding of explosive product gases and deformation even the formation process of fragments. However, the fragments will experience extremely large deformation which could lead to mesh distortion and element entanglement in the Lagrangian finite element method. Although the numerical methods based on Eulerian description can avoid element distortions, it has difficulties such as appropriate representation of free boundary, tracking of the material deformation history and convective terms. The arbitrary Lagrangian-Eulerian (ALE) formulation takes the advantages and alleviates many of the disadvantages both of Lagrangian and Eulerian descriptions [14, 15]. However, designing an efficient and effective mesh-moving algorithm for complicated 3D problems remains a challenging work and the convective terms still pose difficulties in solving equations. Meshfree methods [16–18] use a set of discrete points to construct trial functions. Thus, the problems arising from mesh distortion and element entanglement can be avoided or alleviated. Nevertheless, most of the meshfree methods suffer from higher computational cost and the accuracy of some meshfree methods is still dependent on the node regularities to some extent. Therefore, only a few of them have successfully application in hypervelocity impact problems and explosion problems, such as the smoothed particle hydrodynamics (SPH) [19,20], hybrid particle-element method [21–23].

The material point method (MPM) [24,25] is an extension of the particle in cell (PIC) method called FLIP (Fluid-Implicit-Particle) [26,27] to solid mechanics. It is a fully Lagrangian particle method in which a material domain is discretized with a set of material points (particles) that carry all state variables such as mass, displacement, strain, stress as well as material parameters and internal variables needed for constitutive models. So the movement of the particles represents the movement of the material domain, and the difficulties associated with Eulerian method are completely removed. A regular background grid, which can be fixed in space or moved arbitrarily, is used for solving the momentum equations, so that mesh distortion and element entanglement associated with the traditional Lagrangian finite element method are avoided. Hence, MPM does not require periodical remeshing steps and remapping of state variables, and is therefore better suited to the modeling of

large material deformations. In recent years, much effort has been devoted to the development of MPM. Now MPM and its variants have been successful applied to solve many engineering problems, such as impact [28], penetration [29,30], upsetting problems [28,31], granular media [32], blast induced fragmentation [33–35], problems involved dynamic crack [36–38], fluid–structure interaction problems [39,40], film delamination [41] and so on.

In this paper, the MPM is extended to simulate the explosively driven metal, in which Johnson–Cook material model with Mie–Grüneisen equation of state is implemented to model the behavior of metal with strain rate effect and thermal softening effect taken into consideration, and null material model with Jones–Wilkins–Lee (JWL) equation of state is implemented for describing the expansion process of detonation product gases. Artificial viscosity is added to pressure term to stabilize and capture the shock wave. Two typical explosive/metal configurations, open-faced sandwich and flat sandwich, are analyzed in detail using MPM and numerical results are compared with Gurney solution and its corrections. Based on the numerical results, a correction to Gurney solution is proposed to account for the lateral effects for flat sandwich configuration.

This paper is organized as follows. The explicit material point method is described in Section 2, while the material model and equation of state used are presented in Section 3. The explosively driven metal is analyzed in detail using the 3D explicit material point method in Section 4. Both flat sandwich and open-faced sandwich are analyzed for one-dimensional and two-dimensional configurations with planar symmetry assumption. Finally, several conclusions are given in Section 5.

2. Brief review of material point method

With the updated Lagrangian description, the movement of the continuum domain is governed by the following equation:

Conservation of mass:

$$\rho(X, t)J(X, t) = \rho_0(X) \quad (1)$$

Conservation of momentum:

$$\frac{\partial \sigma_{ji}}{\partial x_j} + \rho f_i = \rho \ddot{u}_i \quad (2)$$

Energy equation:

$$\rho \dot{e} = D_{ij} \sigma_{ij} \quad (3)$$

Constitutive equation:

$$\sigma^{\nabla} = \sigma^{\nabla}(D_{ij}, \sigma_{ij}, etc) \quad (4)$$

Rate of deformation:

$$D_{ij} = \frac{1}{2} \left(\frac{\partial v_i}{\partial x_j} + \frac{\partial v_j}{\partial x_i} \right) \quad (5)$$

Boundary condition:

$$\begin{cases} (n_j \sigma_{ij})|_{\Gamma_t} = \bar{t}_i \\ v_i|_{\Gamma_v} = \bar{v}_i \end{cases} \quad (6)$$

Initial condition:

$$\dot{u}(X, 0) = \dot{u}_0(X), u(X, 0) = u_0(X) \quad (7)$$

where the subscripts i and j denote the component of the space with Einstein summation law, Γ_t the prescribed traction boundary, Γ_u the prescribed displacement boundary, σ_{ij} the Cauchy stress,

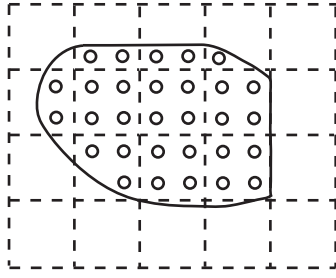


Fig. 1. Material point discretization.

e the energy per unit mass, ρ the current density, f_i the body force per unit mass, \ddot{u}_i the acceleration. The comma denotes covariant differentiation, and n_j is the unit outward normal to the boundary. The conservation of mass is satisfied automatically in Lagrangian description. Taking the virtual displacement δu_i as test function, the weak form of momentum equation can be obtained by the weighted residual method as follows:

$$\int_{\Omega} \rho \ddot{u}_i \delta u_i d\Omega + \int_{\Omega} \rho \sigma_{ij}^s \delta u_{i,j} d\Omega - \int_{\Omega} \rho f_i \delta u_i d\Omega - \int_{\Gamma_t} \rho \bar{t}_i^s \delta u_i d\Gamma_t = 0 \quad (8)$$

where $\sigma_{ij}^s = \sigma_{ij}/\rho$ is the specific stress, $\bar{t}_i^s = \bar{t}_i/\rho$.

The material domain is discretized with a set of particles in MPM, as shown in Fig. 1, so that the density can be approximated as:

$$\rho(x) = \sum_{p=1}^{n_p} m_p \delta(x_i - x_{ip}) \quad (9)$$

where n_p denotes the total number of particles, m_p the mass of particle p , x_{ip} the coordinate of particle p in i th direction, δ the Dirac delta function. Substituting Eq. (9) into the weak form Eq. (8) yields:

$$\sum_{p=1}^{n_p} m_p \ddot{u}_{ip} \delta u_{ip} + \sum_{p=1}^{n_p} m_p \sigma_{ijp}^s \delta u_{ijp} - \sum_{p=1}^{n_p} m_p f_{ip} \delta u_{ip} - \sum_{p=1}^{n_p} m_p \bar{t}_{ip}^s h^{-1} \delta u_{ip} = 0 \quad (10)$$

where $u_{ip} = u_i(x_p)$, $\delta u_{ijp} = \delta u_{i,j}(x_p)$, $\sigma_{ijp}^s = \sigma_{ij}^s(x_p)$, $f_{ip} = f_i(x_p)$, $\bar{t}_{ip}^s = \bar{t}_i^s(x_p)$, and h denotes the thickness of the layer of the boundary.

In MPM, the momentum Eq. (10) is integrated on the background grid. During this phase of solution (Lagrangian solution phase), the particles are rigidly attached to the background grid and they deform with the grid. Therefore, the displacements of particles and their derivatives can be obtained from the grid nodal displacements u_{il} via the standard FE shape functions as

$$u_{ip} = \sum_{l=1}^{n_g} N_{lp} u_{il} \quad (11)$$

Table 2
Material constants of the flyer plate.

$\rho/g \text{ mm}^{-3}$	E/MPa	ν	A/MPa	B/MPa	n
0.0078	200000	0.3	300	200	0.5

$$u_{ip,j} = \sum_{l=1}^{n_g} N_{lp,j} u_{il} \quad (12)$$

where $N_{lp} = N_l(x_p)$ is the value of shape function of grid node l evaluated at particle p . n_g denotes the total number of grid nodes. For three-dimensional cases, 8-node hexahedral grid is adopted as the background grid whose shape functions are given by

$$N_l = \frac{1}{8}(1 + \xi \xi_l)(1 + \eta \eta_l)(1 + \zeta \zeta_l) \quad l = 1, 2, \dots, 8 \quad (13)$$

where (ξ_l, η_l, ζ_l) , either -1 or $+1$, denote the nature coordinates of node l . (ξ, η, ζ) , which are between -1 and $+1$, denote the nature coordinates of a particle. If the particle is outside the hexahedron, $N_l(x_p)$ is equal to zero.

Substituting Eq. (11) and (12) into the Eq. (9) and invoking the arbitrariness of δu_{il} yields:

$$\dot{p}_{il} = f_{il}^{\text{int}} + f_{il}^{\text{ext}} \quad l = 1, 2, \dots, n_g \quad (14)$$

where

$$p_{il} = m_l v_{il} \quad (15)$$

is the momentum of grid node l , and

$$m_l = \sum_{p=1}^{n_p} m_p N_{lp} \quad (16)$$

is the mass of grid node l obtained by mapping the masses of particles located in the cells connected to grid node l ,

$$f_{il}^{\text{int}} = - \sum_{p=1}^{n_p} N_{lp,j} \sigma_{ijp}^s \frac{m_p}{\rho_p} \quad (17)$$

is the internal force of grid node l ,

$$f_{il}^{\text{ext}} = \sum_{p=1}^{n_p} N_{lp} m_p f_{ip} + \sum_{p=1}^{n_p} N_{lp} \bar{t}_{ip}^s h^{-1} \frac{m_p}{\rho_p} \quad (18)$$

is the grid nodal external force.

It can be concluded from above formulations that the material point method is very similar to the traditional FE method. There are two fundamental differences between FEM and MPM. Firstly, the Gauss points are taken as the quadrature points in FEM, while the particles are taken as the quadrature points in MPM. Secondly, the grid is embedded in and deforms with the material domain in

Table 1
Material constants of the TNT explosive.

$A(\text{MPa})$	$B(\text{MPa})$	R_1	R_2	ω	$E_0(\text{MJ} \cdot \text{mm}^{-3})$
372100	3210	4.15	0.95	3	6.993

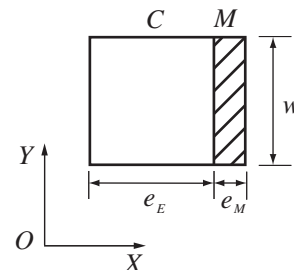


Fig. 2. Initial geometry for an open-faced sandwich.

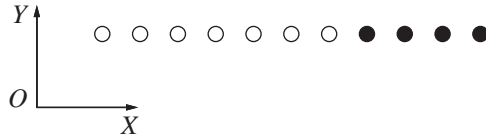


Fig. 3. One-dimensional model for infinite plate case. Hollow dots denote the explosive particles, while solid dots denote the steel particles.

FEM. However, the regular grid is embedded in and deform with the material domain only in the Lagrangian solution phase in MPM, after which the deformed grid is discarded, and a new regular grid is generated for the next time step. Therefore, no permanent information is stored in the grid nodes. The first difference is one of the sources of error in the employment of MPM. For small deformation problems, MPM using of material point integral can be seen as a special FE method, but its accuracy is less than FEM because the material points are not always in the position of Gauss points as simulations evolve. Even in the problem involving large deformation, this error still exists, but may be ignored compared with that resulted from the remeshing in FEM. A detailed analysis of the quadrature error and other error in MPM is given in [42,43].

As a particle method with a background grid, MPM shares some common points with SPH, but it does not suffer from tensile instability existed in SPH. The grid nodes in MPM serve as field nodes to construct the approximation functions of the field variables, whereas the particles serve as quadrature points. Usually, the number of particles is much greater than that of the grid nodes, so that the numerical instability arisen from insufficient quadrature points is avoided [44]. However, there are numerical noise due to particle crossing cell boundary and numerical fracture due to particles separated by a grid cell. Bardenhagen et al [45] proposed a general interpolation material point method (GIMP) to suppress the noises, while Ma et al [46] proposed an adaptive particle splitting scheme to suppress the numerical fracture.

3. Material models

3.1. High explosive model

Based on the Chapman-Jouguet theory, an ideal detonation includes two processes, which are the steady-state detonation process and the following process including expansion of gaseous products and its interaction to the surrounding material. The steady-state detonation can be seen as a shock wave moving through the explosive, whose front compresses and heats the explosive to initiate chemical reaction. Because the velocity of the detonation wave is very fast, the exothermic reaction is completed within few microseconds. The energy released by the reaction feeds the shock front and drives it forward. At the same time, the gaseous products are expanding and interact to the surrounding material. The shock front, chemical reaction, and the leading edge of the rarefaction are all in equilibrium, so they are all traveling at the same velocity, which are named the detonation velocity that is one of material constants of specified explosive [3].

In the initialization phase, a lighting time t_L is calculated for each particle by dividing the distance from the detonation point by the detonation velocity D . If multiple detonation points are specified,

Table 3
Terminal velocity of the metal with different resolutions.

particle space (mm)	0.8	0.4	0.2	0.1	0.04
cell size in x direction (mm)	4	2	1	0.5	0.2
terminal velocity (mm/ms)	575	581	589	592	592

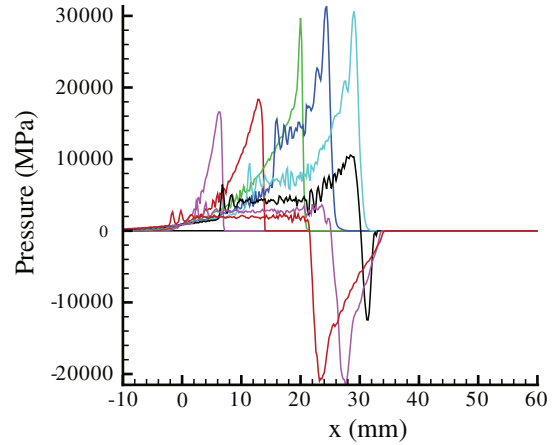


Fig. 4. Pressure profiles along the x direction during the evolution of explosive driving metal.

the closest point determines t_L . After the detonation, the gaseous product is controlled by the equation of state. The real pressure p of the gaseous product is given by multiplying the pressure p_{EOS} obtained from equation of state for explosive with a burn factors F that controls the release of chemical energy for simulating detonation [47]. That is

$$p = F \cdot p_{EOS} \tag{19}$$

where F is the burn factors, which is taken as

$$F = \begin{cases} \frac{(t-t_L)D}{1.5h} & t > t_L \\ 0 & t \leq t_L \end{cases} \tag{20}$$

where h denotes the characteristic size of a particle, and t is the current time. If F exceeds 1, it is reset to 1. It often takes several time steps for F to reach the value 1 by this calculation of the burn fraction. After reaching the value 1, F is held constant. By this method, the discontinuous detonation wave can be smoothed to be a continuous but changing rapidly wavefront in a narrow space.

After detonation, the behavior of gaseous product is governed by the equation of state. Jones-Wilkins-Lee (JWL) equation of state [3] is widely used for describing the detonation products which is given as.

$$p = A \left(1 - \frac{\omega}{R_1 V}\right) e^{-R_1 V} + B \left(1 - \frac{\omega}{R_2 V}\right) e^{-R_2 V} + \frac{\omega E}{V} \tag{21}$$

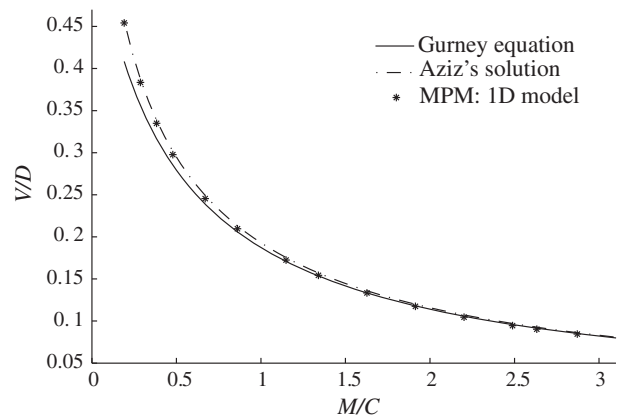


Fig. 5. Dimensionless terminal velocity of metal as a function of M/C for 1D open-faced sandwich.

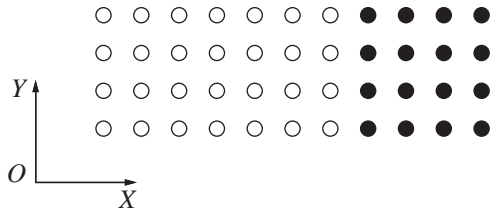


Fig. 6. Two-dimensional model for plate with finite width. The hollow dots denote explosive particles, while the solid dots denote steel particles.

where A, B, R_1, R_2 and ω are the material constants for specified explosive, $V = v/v_0$ is the relative volume, and $E = \rho_0 e$ is the internal energy per initial volume.

Furthermore, this model is always combined with the null material model in which the material strength is often neglected.

3.2. Johnson Cook material model

The Johnson-Cook material model [48] takes into account the effects of strain rate and temperature, and has been widely used to model the behavior of metal in impact and explosion simulation. The yield stress is given by

$$\sigma_y = (A + B\varepsilon^{p^n}) (1 + \text{Cln}\dot{\varepsilon}^*) (1 - T^{*m}) \quad (22)$$

where A, B, n and m are the material constants, ε^p is the effective plastic strain, $\dot{\varepsilon}^*$ denotes the dimensionless effective plastic strain rate and defined as $\dot{\varepsilon}^* = \dot{\varepsilon}^p/\dot{\varepsilon}_0$ for $\dot{\varepsilon}_0 = 1\text{s}^{-1}$, and T^* is the homologous temperature, which is defined as $T^* = (T - T_{\text{room}})/(T_{\text{melt}} - T_{\text{room}})$ with T_{melt} the melt temperature and T_{room} the room temperature.

A simplified Johnson-Cook model can be obtained by ignoring the effect of the temperature in Eq. (22) as

$$\sigma_y = (A + B\varepsilon^{p^n}) (1 + \text{Cln}\dot{\varepsilon}^*) \quad (23)$$

4. Explosive-driven plate problems

In fact, the Gurney model is a one-dimensional model without considering the lateral effects caused by finite lateral dimensions. The Gurney equation may over predict velocities of fragments with large M/C values [8] and underestimate velocities of fragments with relatively lower M/C [3]. In order to investigate the influence of lateral effects, two types of computational model, one-dimensional model representing an infinite plate case and two-dimensional model with planar symmetry assumption representing a finite

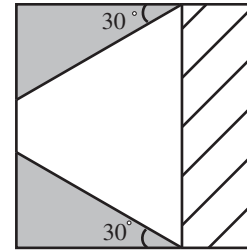


Fig. 8. Discounting angle to account for lateral release of explosive pressure. Shaded region of explosive is discounted.

plate case, are studied using MPM for two typical configurations, open-faced sandwich and flat sandwich, respectively. The termination of the simulation time is set to be long enough to make sure the process of acceleration is completed. The terminal velocities of plates are obtained by averaging particles velocities over the whole plate.

The explosive is TNT whose density $\rho = 1.63\text{g/cm}^3$, detonation velocity $D = 6930\text{ m/s}$, and Gurney characteristic velocity $\sqrt{2E} = 2370\text{ m/s}$. The JWL equation of state is used to model the behavior of detonation products whose material constants are listed in Table 1. The flyer plate driven by TNT explosive consists of steel which is modeled by the simple John-Cook model with material constants listed in Table 2.

4.1. Open-faced sandwich configuration

An open-faced sandwich (metal-explosive assemblage) as shown in Fig. 2 is studied. The whole sandwich of width w consists of one metal plate of thickness e_M and an explosive flat of initial thickness e_E . The Gurney equation for this configuration is expressed as [2]:

$$V = \sqrt{2E} \left[\frac{3}{1 + 5(M/C) + 4(M/C)^2} \right]^{\frac{1}{2}} \quad (24)$$

where V denotes the metal plate velocity, M the mass of the metal plate, C the mass of the explosive, $\sqrt{2E}$ the Gurney characteristic velocity.

4.1.1. One-dimensional model

The plate with infinite width driven by detonation can be modeled by a one-dimensional model, in which only one layer of background grid is used in y and z directions with one layer of particles along the center line of the grid, as shown in Fig. 3. The top, bottom, front and back sides of the grid are set to be symmetrical boundaries and the left and right sides of the grid are

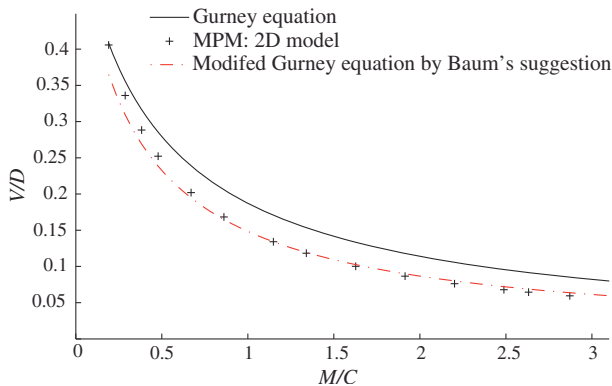


Fig. 7. Dimensionless terminal velocities of metal as a function of M/C for 2D open-faced sandwich configuration.

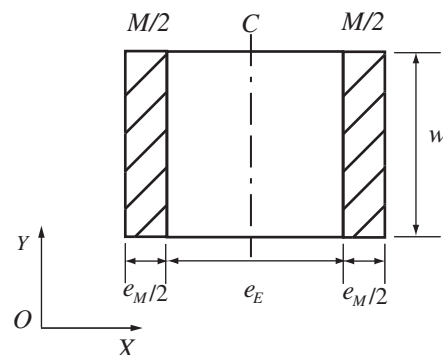


Fig. 9. Initial geometry for a flat sandwich configuration.

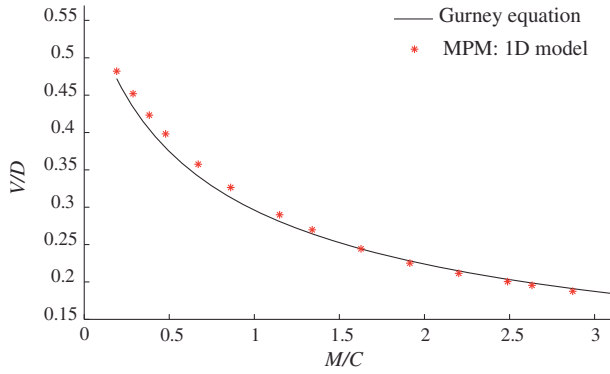


Fig. 10. Dimensionless terminal velocities of metal as a function of M/C for 1D flat sandwich configuration.

set to be traction free boundaries. The thickness of the TNT is 20 mm.

In order to investigate the effects of different particle and cell resolutions, different particle space and cell size are used in the simulation for the flyer plate with thickness of 12 mm and $M/C = 2.8712$. The numerical results are listed in Table 3, which shows that numerical terminal velocity converges to the prediction of Gurney equation.

The shock wave is an important feature in the evolution of explosive driving metal. To investigate the propagation of shock wave, this one-dimensional problem is studied with particle space 0.04 mm. According to the detonation velocity, it takes about 2.886 μ s to complete the detonation. Hence, Fig. 4 plots the pressure profile along the x direction at 1 μ s interval from 0 to 8 μ s. The pressure peak is close to the C-J pressure 1.957×10^4 MPa [49] by the preceding two curves. Once the detonation wave meets the interface between detonation product and flyer, transmitted wave and reflected wave are generated. Because wave impedance of steel is greater than that of detonation product with transmission coefficient greater than 1, the pressure peak of the transmitted wave is greater than that of the incident wave. Tensile wave is induced by the reflection of the compressive waves at the free surface of the flyer plate.

Based on the results of convergence test listed in Table 3, uniform particles with space of 0.1 mm and uniform background grid with cell sizes of 0.5 mm \times 0.5 mm \times 0.5 mm are used in following simulations. The thickness of the flyer plate is determined by the ratio of M/C . So the TNT is modeled with 200 particles, while the number of particles for modeling plate is from 8 to 68,

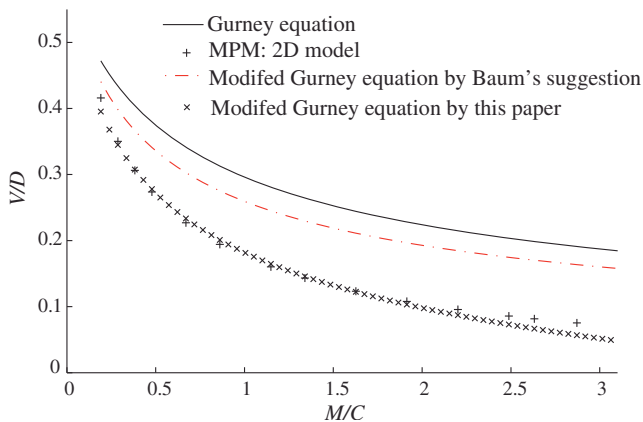


Fig. 11. Dimensionless terminal velocities of metal plate as a function of M/C for 2D flat sandwich configuration.

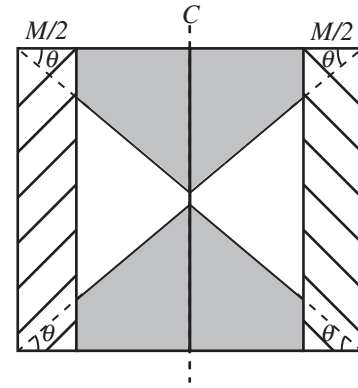


Fig. 12. Discounting angle to account for lateral release of explosive pressure. Shaded region of explosive is discounted.

according to the different thickness of the plate. The explosive is in the left of the metal plate, and the detonation ignites from the left side of the explosive by defining a detonation point at the left side of the explosive with lighting time 0.

The terminal velocities of metal obtained by MPM for various values of M/C are compared with the prediction of Gurney equation in Fig. 5. As shown in Fig. 5, the numerical results obtained by MPM agree very well with the prediction of Gurney equation for large values of M/C , but they deviate at small values of M/C . Gurney models are over simplified for low values of M/C where gas-dynamic behavior dominates, so that Gurney solutions cannot be trusted for this regime. By modeling the driven metal as a rigid body and the gases with an ideal gas equation of state, Aziz et al. obtained the terminal velocity for an open-faced sandwich configuration as [13]

$$\frac{V}{D} = 1 - \frac{27}{16} \frac{M}{C} \left[\left(1 + \frac{32}{27} \frac{C}{M} \right)^{1/2} - 1 \right] \quad (25)$$

where D is the detonation velocity of explosive. This solution should be applicable for all values of M/C because it treats the gas dynamics fully. Fig. 5 shows that MPM solution agree very well with Aziz's solution given by Eq. (25). Therefore, MPM can be used to analyze the explosively driven metal with all values of M/C .

4.1.2. Two-dimensional model

In order to estimate the influence of the lateral effects on terminal velocity of the metal plate, a two-dimensional model with plate of infinite length and finite width is studied. Considering the symmetry of the model, half of the domain is modeled. Only one layer of the background grid is set in z direction with one layer of particles in the center plane of the grid, as shown in Fig. 6. The left, right and upper sides of the grid are free boundaries, while the bottom, front and back sides of the grid are symmetrical boundaries. The thickness of the explosive is 10 mm and the width 20 mm. The thickness of the metal plate is determined by the ratio of M/C . All other parameters are the same as that used in the

Table 4
The number of particles of discrete models used in the simulations for $M/C = 1.9141$.

w/e value	100	50	100/3	25	20	50/3
particles TNT	200 \times 10	100 \times 10	100 \times 15	50 \times 10	40 \times 10	50 \times 15
number Plate	200 \times 4	100 \times 4	100 \times 6	50 \times 4	40 \times 4	50 \times 6
w/e value	12.5	10	25/3	20/3	50/9	
particles TNT	50 \times 20	50 \times 25	25 \times 15	40 \times 30	50 \times 45	
number Plate	50 \times 8	50 \times 10	25 \times 6	40 \times 12	50 \times 18	

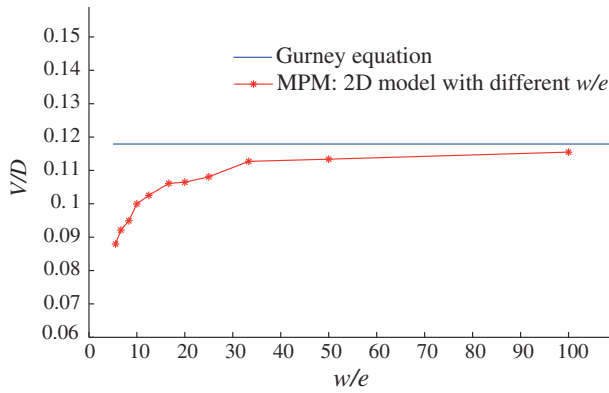


Fig. 13. Dimensionless velocity of metal plate as a function of w/e for 2D open-faced sandwich for $M/C = 1.9141$.

one-dimensional model. Here, the TNT is modeled with 10000 particles, while the number of particles for modeling plate is from 400 to 3400 according to the thickness of the plate. A detonation line is defined at the left side of the explosive with lighting time 0.

The terminal velocities of metal obtained by MPM are compared with Gurney prediction in the Fig. 7. For small values of M/C , the solutions overlay well. At large values of M/C , the solutions deviate, with the Gurney equation predicting higher velocities than the MPM results. The Gurney assumptions are so simplified that it cannot handle the lateral effects which played an important role in reducing the terminal velocity of flyer plate. That is to say, the Gurney model is generally applied for one-dimensional configuration. This example is two-dimensional and there is rarefaction wave coming from the free boundary which affected a special zone of detonation product gases that did not contribute to the momentum of the plate [3]. When M increasing, the time taken for the metal plate to reach its final velocity increases and so there is more time for the lateral rarefaction to take place and reduce the terminal velocity of the plate [9]. Therefore, the prediction of Gurney model is overestimated for two-dimensional and three-dimensional configurations. In order to use Gurney model for two-dimensional problems, the model is needed to be improved to considering the effects of the rarefaction wave. Baum et al. [11] suggested subtracting a part of explosive from the total mass C to take into account the lateral effects. For the open-faced sandwich configuration shown in Fig. 8, Kennedy estimated that the explosive, which should be subtracted from the total mass C , was that

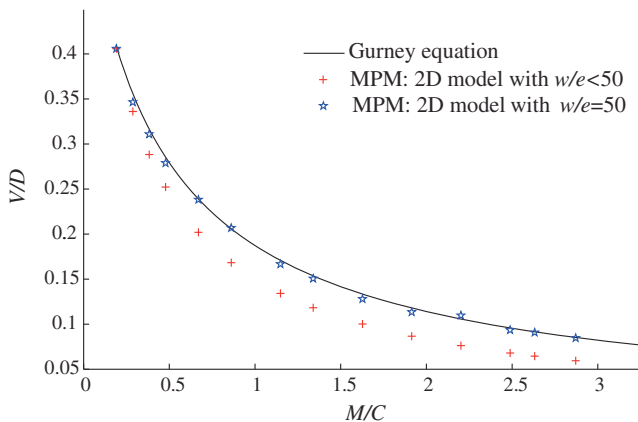


Fig. 14. Comparison of MPM solution with Gurney solution for 2D open-faced sandwich for $w/e = 50$.

Table 5

The number of particles of discrete models used in the simulations for $w/e = 50$.

M/C value		0.1914	0.2871	0.3828	0.4785	0.6699
particles	TNT	100×100	75×50	100×50	100×40	175×50
	Plate	100×4	75×3	100×4	100×4	175×7
M/C value		0.8613	1.1485	1.3399	1.6270	1.9141
particles	TNT	225×50	150×25	175×25	170×20	100×10
	Plate	225×9	150×6	175×7	170×7	100×4
M/C value		2.2012	2.4883	2.6319	2.8712	
particles	TNT	275×25	325×25	275×20	300×20	
	Plate	275×11	325×13	275×11	300×12	

outside the boundary of an angle of 30° to a normal to the plate [3], and the value of the angle seems to produce the best correlation with experiments results. Based on this suggestion, the prediction of Gurney equation is modified and the results are also plotted in Fig. 7, which agree well with the MPM results.

4.2. Flat sandwich configuration

From the above examples, the prediction for open-faced sandwich configuration by MPM shows good agreement with that of Gurney equation and improved Gurney equation. Then, a flat sandwich, which is a symmetric metal-explosive-metal system as shown in Fig. 9, is studied for one-dimensional configuration and two-dimensional configuration. The Gurney equation for flat sandwich is given as

$$V = \sqrt{2E} \left(\frac{M}{C} + \frac{1}{3} \right)^{-\frac{1}{2}} \tag{26}$$

4.2.1. One-dimensional model

Considering the symmetry, only one half of the metal-explosive-metal system is modeled. All parameters for the model are the same as that in the one-dimensional model for open-faced sandwich, as shown in Fig. 3, but the left side of the grid is symmetrical boundary and the thickness of TNT is 20 mm. And the TNT is modeled with 200 particles, while the number of particles for modeling plate is from 8 to 68 according to the size of the plate. The detonation ignites from the center of the explosive by defining a detonation point at the left side of the grid with lighting time 0. The terminal velocities of the metal obtained by MPM for various values of M/C agree very well with the predictions of Gurney equation as shown in Fig. 10.

4.2.2. Two-dimensional model

One quarter of the metal-explosive-metal system is modeled due to the symmetry. Only one layer of the background grid is set in z direction. The front, back, bottom and left sides of the grid are

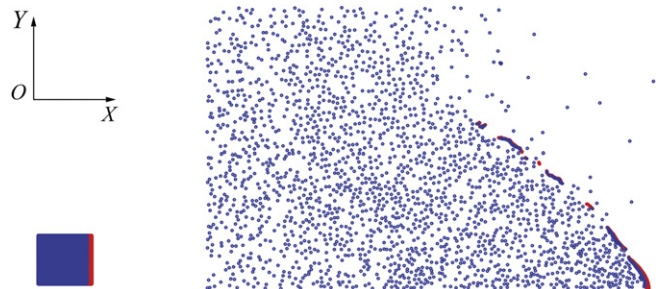


Fig. 15. The initial configuration (left) and the configuration of an open-faced sandwich with $M/C = 0.4785$ at 0.06 ms after detonation (right).

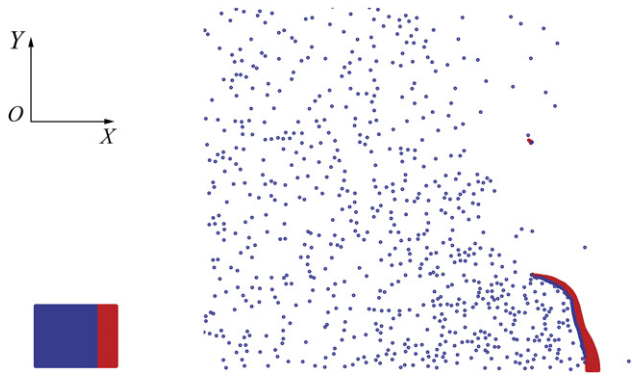


Fig. 16. The initial configuration (left) and the configuration of an open-faced sandwich with $M/C = 1.6270$ at 0.1 ms after detonation (right).

symmetric boundaries, while the right and upper sides are free boundaries. The thickness of the plate is 10 mm and width 20 mm. The thickness of the metal is determined based on the values of M/C . All other parameters are the same as that in the 2D open-faced sandwich model, and the material point discretization for the 2D flat sandwich model is the same as that shown in Fig. 6. Here, the TNT is modeled with 10000 particles.

The numerical results obtained by MPM are compared with the prediction of Gurney equations in Fig. 11, which shows that the solutions deviate seriously. Undoubtedly, the lateral effects will be significant for plate with finite lateral dimensions, so that the Gurney equation will over predict the terminal velocities. Therefore, it is necessary to modify Gurney equation for this configuration. However, Kennedy's estimation of 30° still overpredicts significantly the terminal velocities for this configuration as shown in Fig. 11. Considering that Baum's correction is a very simple and convenient way to account for the lateral effects in engineering, we attempted to adjust the angle of the boundary outside which the explosive are subtracted from the total mass C , and found that the angle of 45° , as shown in Fig. 12, seems to produce the best correlation with the MPM results, see Fig. 11.

4.2.3. The influence of metal plate sizes

Above results indicate that the lateral effects play an important role to reduce the terminal velocities of the flyer plate in two-dimensional models. However, the lateral effects on the terminal velocities should decrease with increase of the width w of plate, so that the results of two-dimensional model should be converged to those of one-dimensional model if the ratio of plate width w to plate thickness e is large enough.

Therefore, a set of simulations for 2D open-faced sandwich for various values of w/e at a constant value of $M/C = 1.9141$ were done. Half of the domain is modeled due to symmetry with the particle space 0.1 mm. All the discretized parameters are same to above, and the total number of particles for the models is listed in Table 4. Fig. 13 compares the terminal velocities of the metal plate obtained by MPM with the Gurney solutions, and shows that the MPM results for 2D model approach to the Gurney solution when w/e increases, and they agree well after $w/e > 50$.

A group of samples of 2D open-faced sandwich with constant width-to-thickness ratio of 50 are studied by MPM, and their results are compared with the Gurney solutions in Fig. 14. And the number of particles used in this set simulations is listed in Table 5 for half model with particle space 0.1 mm. The MPM results for $w/e = 50$ agree very well with the Gurney solution, because the mass discounted for this case is neglected compared with the total mass of the explosive.

4.2.4. The deformation of the system

It is easy to notice that the Gurney equation can only predict the terminal velocity of the plate for some simple cases. In contrast, MPM provides a powerful tool for studying the whole process of the explosively driven flyer problems, including the expanding of explosive product gases and deformation even the formation process of fragments. Figs. 15 and 16 illustrate the configuration of an open-faced sandwich with $M/C = 0.4785$ and $M/C = 1.6270$ at 0.06 ms and 1 ms after detonation, respectively. As shown in these figures, the flyer plate experiences large deformation and the product of detonation expands violently. When the ratio of mass is low, the flyer plate is easy to fracture in width direction, which is due to the fact that detonation wave is not a plane wave that will strengthen the rarefaction wave in the corner of the flyer plate.

5. Conclusion

In this paper, the material point method is extended to simulate the explosively driven metal, in which Johnson-Cook material model with Mie–Grüneisen equation of state is used to model the behavior of metal, and null material model with Jones-Wilkins-Lee (JWL) equation of state is used for describing the expansion process of detonation product gases. Two typical configurations, open-faced sandwich and flat sandwich, are studied using MPM for various values of M/C and numerical results are compared with Gurney solution and its corrections.

The Gurney solution is actually obtained based on one-dimensional assumption. Hence, the Gurney solutions agree very well with the MPM results for one-dimensional configurations. However, the Gurney solution gives overestimated final velocity of flyer plate for two-dimensional configurations because it neglects the lateral effects which plays an important role in reducing the terminal velocity of flyer plate. For open-faced sandwich configuration, Kennedy's estimation of 30° produces the best correlation with experiments results, but still over predicts significantly the terminal velocities for flat configuration. Our MPM study suggests that the angle of 45° as shown in Fig. 12 seems to produce the best correlation with the MPM results.

This study suggests that MPM provides a powerful tool for studying the explosively driven plates and other related explosive problems.

References

- [1] Gurney RW. The initial velocities of fragments from bombs, shells, and grenades. Technical Report A407982. Aberdeen, MD: Ballistic Research Laboratory; September 1943.
- [2] Meyers MA. Dynamic behavior of materials. John Wiley & Sons; 1994.
- [3] Zukas JA, Walters WP. Explosive effects and applications. Springer; 1998.
- [4] Butz DJ, Backofen JE. Fragment terminal velocities from low metal to explosive mass ratio symmetric sandwich charges. J Ballistics 1986;6:1304–25.
- [5] Roth J. Correlation of the gurney formula for the velocity of explosively driven fragment with detonation parameters of the driver plate. Technical Report No. 001.71. Menlo Park, CA: Poulter Laboratory, Stanford Research Institute; 1971.
- [6] Henry JG. The gurney formula and related approximations for the high-explosive deployment of fragments. Technical Report PUB-189. Culver City, CA: Hughes Aircraft Company; 1967. April (AD 813398).
- [7] Kennedy JE. Explosive output for driven metal. In: Davison L, Kennedy JE, Coffey F, editors. Pro. 12th Annual Sym. on Behavior and Utilization of Explosive in Engineering Design. New Mexico, March 2–3 1972. p. 109–124.
- [8] Bol J, Honcia G. Velocity of H.E. accelerated plates for low values of α . In: Schroder GA, editor. 3rd International Symposium on Ballistics, Karlsruhe, Germany, 1977.
- [9] Chanteret PY. Velocity of the driven metal plates with finite lateral dimensions. In: Riegel J, Murphy MJ, editors. Proceedings of the 12th International Symposium on Ballistics, San Antonio, TX. National Defense Industrial Association: Washington, DC; 1990. p. 369–378.
- [10] Fucke W, Bol J, Schumann St. Velocity of sandwich plates driven by thin H.E. layers. In: Post JR, editor. Proceedings of the 10th International Symposium on Ballistics, vol. 2, San Diego, USA, 1987.

- [11] Baum FA, Stanyukovich K, Shekhter BI. Physics of an explosions. Moscow (English translation from Federal Clearinghouse AD 400151); 1959.
- [12] Benham RA. Terminal velocity and rotation rate of a flyer plate propelled by a tube-confined explosive charge. Shock Vibration Bull 1979;49:193–201.
- [13] Aziz AK, Hurwitz H, Sternberg HM. Energy transfer to a rigid piston under detonation loading. Phys Fluids 1961;4:380–4.
- [14] Liu WK, Belytschko T, Chang H. An arbitrary lagrangian-eulerian finite element method for path-dependent materials. Comput Methods Appl Mech Engrg 1986;58:227–45.
- [15] Gadala MS, Wang J. ALE formulation and its application in solid mechanics. Comput Methods Appl Mech Engrg 1998;167:33–55.
- [16] Belytschko T, Krongauz Y, Organ D, Fleming M, Krysl P. Meshless methods: an overview and recent developments. Comput Methods Appl Mech Engrg 1996;139(1–4):3–47.
- [17] Li S, Liu WK. Meshfree and particle methods and their applications. Appl Mech Rev 2002;55(1):1–34.
- [18] Liu MB, Liu GR, Lam KY, Zong Z. Meshfree particle simulation of the detonation process for high explosives in shaped charge unlined cavity configurations. Shock Waves 2003;12(6):509–20.
- [19] Liu GR, Liu MB. Smoothed particle hydrodynamics: a meshfree particle method. Singapore: World Scientific; 2003.
- [20] Liu X, Liu GR. Radial point interpolation collocation method for the solution of nonlinear poisson problems. Comput Mech 2005;36(4):298–306.
- [21] Rabb RJ, Fahrenthold EP. Numerical simulation of oblique impact on orbital debris shielding. Int J Impact Eng 1999;23(1):735–44.
- [22] Fahrenthold EP, Horban BA. An improved hybrid particle -element method for hypervelocity impact simulation. Int J Impact Eng 2001;26(1–10):169–78.
- [23] Park YK, Fahrenthold EP. A kernel free particle-finite element method for hypervelocity impact simulation. Int J Numer Meth Engrg 2005;63(5):737–59.
- [24] Sulsky D, Chen Z, Schreyer HL. A particle method for history-dependent materials. Comput Methods Appl Mech Engrg 1994;118(1–2):179–96.
- [25] Sulsky D, Zhou SJ, Schreyer HL. Application of a particle-in-cell method to solid mechanics. Comput Phys Comm 1995;87(1–2):236–52.
- [26] Brackbill JU, Ruppel HM. FLIP: a method for adaptively zoned, particle-in-cell calculations of fluid flows in two dimensions. J Comput Phys 1986;65:314–43.
- [27] Brackbill JU, Kothe DB, Ruppel HM. FLIP: a low-dissipation, particle-in-cell method for fluid flow. Comput Phys Comm 1988;48:25–38.
- [28] Sulsky D, Schreyer HL. Axisymmetric form of the material point method with applications to upsetting and Taylor impact problems. Comput Methods Appl Mech Engrg 1996;139(1–4):409–29.
- [29] Zhang X, Sze KY, Ma S. An explicit material point finite element method for hyper-velocity impact. Int J Numer Meth Engrg 2006;66(4):689–706.
- [30] Wang YX, Chen Z, Zhang HW, Sun M. Response of multi-layered structure due to impact load using material point method. Eng Mechanics 2007;24(12):186–92 [in Chinese].
- [31] Sulsky D, Kaul A. Implicit dynamic in the material-point-method. Comput Methods Appl Mech Engrg 2004;193(12–14):1137–70.
- [32] Bardenhagen SG, Brackbill JU, Sulsky D. The material-point method for granular materials. Comput Methods Appl Mech Engrg 2000;187(3–4):529–41.
- [33] Hu WQ, Chen Z. Model-based simulation of the synergistic effects of blast and fragmentation on a concrete wall using the mpm. Int J Impact Eng 2006;32(12):2066–96.
- [34] Guillkey JE, Harman TB, Banerjee B. An eulerian-lagrangian approach for simulating explosions of energetic devices. Comput Struct 2007;85:660–74.
- [35] Wang YX, Chen Z, Sun M. Simulation of explosion and shock involving multiple materials based on the material point method. Explosion and Shock Waves 2008;28(2):154–60 [in Chinese].
- [36] Guo Y, Nairn JA. Calculation of J integration and stress intensity factors using the material point method. Comput Model Eng Sci 2004;6:295–308.
- [37] Guo YJ, Nairn JA. Three-dimensional dynamic fracture analysis using the material point method. Comput Model Eng Sci 2006;16(3):141–55.
- [38] Ma J, Lu HB, Komanduri R. Structured mesh refinement in generalized interpolation material point (gimp) method for simulation of dynamic problems. Comput Model Eng Sci 2006;12(3):213–27.
- [39] York II AR, Sulsky D, Schreyer HL. Fluid-membrane interaction based on the material point method. Int J Numer Meth Eng 2000;48:901–24.
- [40] Anvar G, Sumanta A. A hybrid immersed boundary and material point method for simulating 3d fluid-structure interaction problems. Int J Numer Meth Fl 2008;56:2151–77.
- [41] Shen LM, Chen Z. A silent boundary scheme with the material point method for dynamic analyses. Comput Model Eng Sci 2005;7(3):305–20.
- [42] Steffen M, Kirby RM, Berzins M. Analysis and reduction of quadrature errors in the material point method (mpm). Int J Numer Meth Eng 2008;76:922–48.
- [43] Wallstedt PC, Guilkey JE. Improved velocity projection for the material point method. Comput Model Eng Sci 2007;19(3):223–32.
- [44] Ma S, Zhang X, Qiu XM. Comparison study of MPM and SPH in modeling hypervelocity impact problems. Int J Impact Eng 2009;36:272–82.
- [45] Bardenhagen SG, Kober EM. The generalized interpolation material point method. Comput Model Eng Sci 2004;5(6):477–95.
- [46] Ma S, Zhang X, Lian YP, Zhou X. Simulation of high explosive explosion using adaptive material point method. Comput Model Eng Sci 2009;39(2):101–23.
- [47] Hallquist JO. ANSYS/LS-DYNA theoretical manual. Livermore Software Technology Corporation; 2006.
- [48] Johnson GR, Cook WH. A constitutive model and data for metals subjected to large strains, high strain rates and high temperatures. In: Hans Pasman, editor. 7th International Symposium on Ballistics, The Hague, Netherlands: American Defense Preparedness Association; 1983. p. 541–547.
- [49] Liu MB, Liu GR, Zong Z, Lam KY. Computer simulation of high explosive explosion using smoothed particle hydrodynamics methodology. Comput Fluids 2003;32(3):305–22.